Journal of Theoretical Biology 430 (2017) 32–44

Contents lists available at ScienceDirect

Journal of Theoretical Biology

journal homepage: www.elsevier.com/locate/jtbi

Modeling coexistence of oscillation and Delta/Notch-mediated lateral inhibition in pancreas development and neurogenesis

Hendrik B. Tiedemann[a], Elida Schneltzer[a], Johannes Beckers[a,b,c], Gerhard K.H. Przemeck[a,b], Martin Hrabě de Angelis[a,b,c,*]

[a] Institute of Experimental Genetics, Helmholtz Zentrum München – German Research Center for Environmental Health, Ingolstaedter Landstr. 1, 85764 Neuherberg, Germany
[b] German Center for Diabetes Research (DZD), Ingolstaedter Landstr. 1, 85764 Neuherberg, Germany
[c] Chair of Experimental Genetics, School of Life Sciences Weihenstephan, Technische Universität München, Alte Akademie 8, 85354 Freising, Germany

ARTICLE INFO

Article history:
Received 18 November 2016
Revised 2 June 2017
Accepted 7 June 2017
Available online 23 June 2017

Keywords:
Pancreatogenesis
Cycling gene expression
Neurog3
Endocrine progenitor
Simulation

ABSTRACT

During pancreas development, *Neurog3* positive endocrine progenitors are specified by Delta/Notch (D/N) mediated lateral inhibition in the growing ducts. During neurogenesis, genes that determine the transition from the proneural state to neuronal or glial lineages are oscillating before their expression is sustained. Although the basic gene regulatory network is very similar, cycling gene expression in pancreatic development was not investigated yet, and previous simulations of lateral inhibition in pancreas development excluded by design the possibility of oscillations. To explore this possibility, we developed a dynamic model of a growing duct that results in an oscillatory phase before the determination of endocrine progenitors by lateral inhibition. The basic network (D/N + Hes1 + Neurog3) shows scattered, stable *Neurog3* expression after displaying transient expression. Furthermore, we included the Hes1 negative feedback as previously discussed in neurogenesis and show the consequences for *Neurog3* expression in pancreatic duct development. Interestingly, a weakened HES1 action on the *Hes1* promoter allows the coexistence of stable patterning and oscillations. In conclusion, cycling gene expression and lateral inhibition are not mutually exclusive. In this way, we argue for a unified mode of D/N mediated lateral inhibition in neurogenic and pancreatic progenitor specification.

1. Introduction

The pancreas as a bifunctional organ releases digestive enzymes from acinar cells to the duodenum and secretes the hormones glucagon, insulin, somatostatin, pancreatic polypeptide and ghrelin from the islets of Langerhans as endocrine part into the blood stream to regulate glucose homeostasis.

The murine pancreas arises around gestational day 9.5 (E9.5) as two epithelial outgrowths, known as the pancreatic buds, on the dorsal and ventral side of the embryonic gut. They are characterized by the expression of the transcriptional factors PDX1 and PTF1A (Jorgensen et al., 2007; Roark et al., 2012). Signals like FGF10 from the surrounding mesenchyme are important for further growth and differentiation (Hart et al., 2003; Norgaard et al., 2003). The growing buds fuse to one organ around E12.5 when the gut has rotated (Jorgensen et al., 2007), whereby 'primary transition', the first phase of pancreas development, ends. During further growth, fluid-filled micro-lumina build an epithelium-lined network of branching ducts growing towards the FGF10 expressing mesenchyme, thereby pushing it away toward the periphery of the arboreal structure (Gittes, 2009). Acinar cells develop at the tip of each branch and are characterized by *Ptf1a*, which is initially expressed in the whole pancreatic epithelium (as *Pdx1, Nkx6-1* and *Sox9*) but becomes restricted to the tips while *Nkx6-1* and *Sox9* are limited to the trunk of the growing ducts (Zhou et al., 2007).

Neurogenin3 (*Neurog3*) encodes a pivotal transcription factor for endocrine cell development (Gradwohl et al., 2000) and is expressed in a scattered pattern throughout the growing epithelial ducts (Rukstalis and Habener, 2009). Tracing experiments gave evidence that *Neurog3* positive (*Neurog3+*) cells are precursors of the endocrine cell lineage (Gu et al., 2003). The fact that not all cells express *Neurog3* is usually explained by Delta-Notch (D/N) mediated lateral inhibition (LI) (Afelik and Jensen, 2013; Jensen, 2004).

* Correspondence author at: Institute of Experimental Genetics, Helmholtz Zentrum München – German Research Center for Environmental Health, Ingolstaedter Landstr. 1, 85764 Neuherberg, Germany.
E-mail address: hrabe@helmholtz-muenchen.de (M. Hrabě de Angelis).

http://dx.doi.org/10.1016/j.jtbi.2017.06.006

Although not proven for pancreas development, there are indications that NEUROG3 induces *Dll1* in the same cell (Castro et al., 2006; Gasa et al., 2004), which encodes a membrane-residing ligand for NOTCH on neighboring cells. Upon binding of DLL1 to NOTCH, the intracellular domain of NOTCH (NICD) is cleaved off and moves to the cell nucleus where it acts as transcriptional activator together with cofactors (Bray, 2006). Among D/N targets are transcription factors of the Hes and Hey family. In particular HES1 is important, whose failure leads to pancreatic hypoplasia as it acts as a negative regulator of endodermal differentiation (Jensen et al., 2000) and serves as a repressor of *Neurog3* (Lee et al., 2001). Thus, a NEUROG3 expressing cell prevents surrounding cells from acquiring the same cell fate. Taking out components of the D/N-pathway results in an excessive number of Neurog3 expressing cells (Apelqvist et al., 1999). Additionally, proliferation in the buds is reduced, as HES1 inhibits proliferation-inhibiting factors, and NEUROG3 cell-autonomously induces the cell-cycle inhibitor *Cdkn1a*, thereby preventing endocrine-progenitor proliferation (Miyatsuka et al., 2011).

During secondary transition, which starts around E12.5 (Pan and Wright, 2011; Shih et al., 2013), ever more cells of the growing ducts become *Neurog3*+ and restrict other cells to the ductal fate by D/N-signaling (Pan and Wright, 2011). Downstream of NEUROG3, endocrine precursor cells express *Snail2* (Rukstalis and Habener, 2007), a master controller of epithelial to mesenchymal transition (EMT) (Yu et al., 2015), which results in the delamination of *Neurog3*+ cells from the epithelial duct and their migration into the mesenchyme where they initiate the formation of the islets of Langerhans.

As *Neurog3*+ cells are the progenitors of all endocrine cell types (Gu et al., 2002; Rukstalis and Habener, 2009), elucidating the underlying mechanisms leading to their generation is of utmost importance in respect to stem-cell replacement therapies for diabetes. In this context, the following questions are of special interest: (i) which signal transduction pathways lead to the differentiation of a pancreatic progenitor cell from an endodermal cell, (ii) in which time course and how is the ratio of *Neurog3* positive to negative cells established, and (iii) which mechanisms ensure the division of the pancreatic epithelium into tip and trunk region and the differentiation into duct and endocrine progenitors?

Although the *in vivo* situation is far more complex (Bankaitis et al., 2015) theoretical modeling could be valuable for a better understanding of these processes. However, compared to other developmental processes only very few theoretical models describe aspects of pancreas development. De Back et al. (2013) modeled LI in a static (non-growing) two-dimensional hexagonal cell lattice to predict an assumed ratio of *Neurog3*+ to duct cells, and Zhou et al. (2011) described the differentiation of a single progenitor cell into islet-cell types by a hierarchical gene regulatory network (GRN) of mutual inhibitory transcription factors.

Here, we employed a multi-cellular compartment model that describes oscillatory gene expression in a growing pancreatic duct to examine the temporal development of *Neurog3* expression in endocrine progenitors during secondary transition of pancreas development. Using the gene interactions described above the model predicts an oscillatory phase of *Neurog3* expression before its stabilization in a 1:2 pattern of positive to negative duct cells. The temporal progression of differentiation in the growing duct is translated into a spatial difference between a part rich in stable *Neurog3*+ cells distant to the growth zone and a part near the growth zone with oscillatory *Neurog3* expression (see Fig. 1 for a graphical abstract).

Additionally, we modeled LI by using a network where HES1 inhibits not only *Neurogenin* but also directly *Dll1* (Kobayashi and Kageyama, 2014) and observed a similar behavior. However, experimentally observed oscillations in neurogenesis have periods of 2–3 h (Shimojo et al., 2008), which was interpreted as consequence of the negative feedback of HES1 on its gene promoter (Shimojo et al., 2011). Including this feedback into our GRN resulted in stable *Neurog3* expression after transient oscillations only when the susceptibility of the *Hes1* promoter for HES1 binding was weakened. We therefore postulate a mechanism where HES1-binding to its own promoter is diminished by ID (inhibitor of DNA binding) proteins induced by BMP4 signaling. In this way, one could formulate a unified model of progenitor cell determination for neurogenesis and pancreas development.

2. Results

2.1. Model setting and scope

We do not model duct formation by epithelialization and self-organization from the pancreatic bud (Villasenor et al., 2010). Cell movement, contact inhibition and proliferation are introduced phenomenologically to set boundary conditions for the pattern-generating GRN, whereas cell deformation, cell adhesion and cell-cell forces are not included. In this way, cells divide in a user-defined growth zone at the tip of the growing duct and, when delamination is allowed, inside the duct to fill a void left by a delaminating cell. The user-defined growth rate is fixed and not based on a cell-cycle model. Daughter cells are placed on a growing hexagonal lattice to the tube depending on their growth (cell division) direction. They can adopt concentration values of their mother cells when this option is chosen. Daughter cells gradually move into place in user-defined 'growth steps', which implicitly sets the growth rate.

EMT triggered by *Snail2* (Gouzi et al., 2011) is modeled only phenomenologically. When delamination is active, a cell that attained a certain concentration of SNAIL2 starts a random walk out of the duct. The resulting gap is filled by the proliferation of its mother cell. However, we ignored *Snail2* induction in most of our simulations to avoid that the typical pattern of one *Neurog3*+ cell surrounded by *Neurog3*– cells is harder to discern when we allow proliferation after EMT. We therefore restricted our model to an augmented proliferation at the tip, since the probability and distribution of proliferation along the duct is still unknown. Furthermore, our 'cells' are incompressible spheres. A proliferation in the duct outside of the growth zone would result in the cells pushing each other further and further, thereby disturbing a large part of the D/N connections. By restricting the proliferation inside the duct only to 'replacement proliferation' after delamination our simulations are not realistic in respect to growth processes.

Excluding branching, the model is intended to simulate one pancreatic duct growing towards an assumed FGF10 secreting mesenchyme that is pushed by the growing duct to the periphery (Gittes, 2009), whereby the influence of FGF10, or another yet unknown growth-promoting factor (as FGF10 seems to be not expressed after E11.5 (Bhushan et al., 2001)), becomes weaker.

2.2. The models

We developed a variant of the cell- and gene-based simulation tool as described recently (Tiedemann et al., 2012). The basic GRN in each virtual cell comprises *Neurog3, Hes1, Delta1*, and *Notch1* (Fig. 2A). Oscillations are generated by a negative feedback of HES1 onto the *Neurog3* promoter with delay, as NEUROG3 induces DLL1, which binds to NOTCH1 on a neighboring cell and triggers the release of the NICD that induces the transcription of *Hes1*. Our model explicitly involves the transport of proteins and mRNAs between the nucleus and the cytoplasm, i.e. we use a so-called compartment model. To explore consequences of

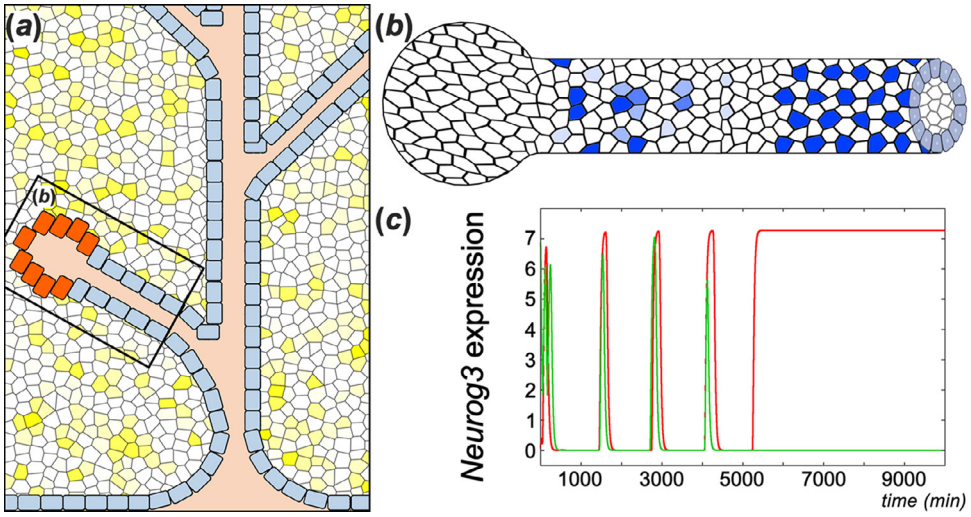

Fig. 1. Graphical abstract. (A) Pancreatic ducts growing into the surrounding mesenchyme. (B) One duct with a growing tip and *Neurog3* expressing cells (blue) in the trunk. (C) Time course of *Neurog3* mRNA concentration for two neighboring cells. After their origin in the growth zone, both cells oscillates in the vicinity of the growing tip before they differentiate into distinctive fates with the red cell stabilizing at high and the green cell at low *Neurog3* concentrations.

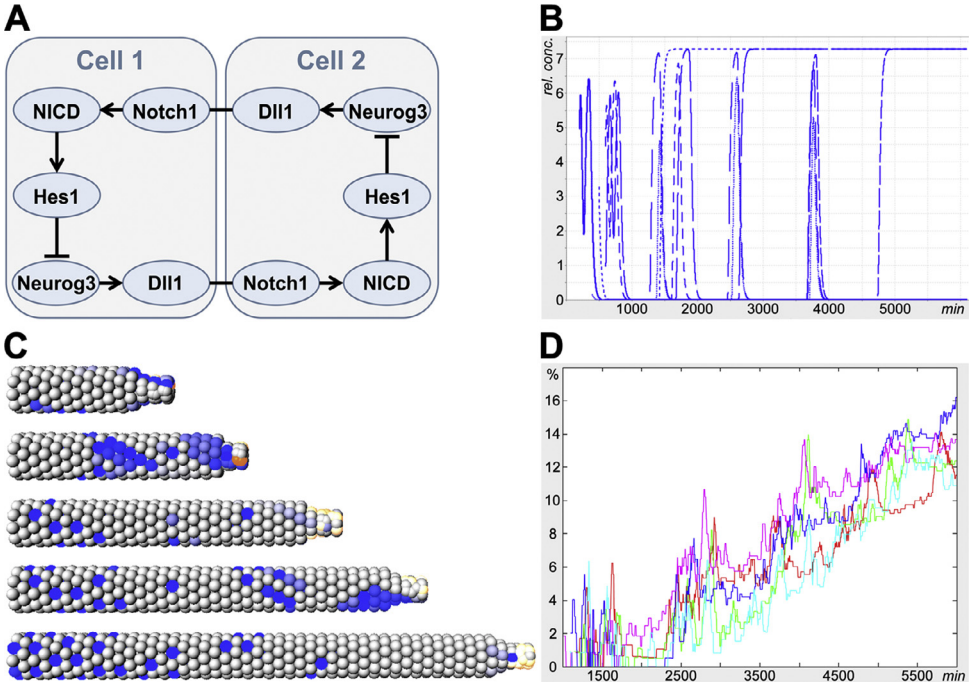

Fig. 2. Simulation result for the standard GRN in which NEUROG3 activates *Dll1* and HES1 inhibits *Neurog3*. The noise is introduced by a transcription stop during mitosis and standard parameters were used (Table S1). The Hill functions and -thresholds are described in Table S2. (A) Reaction scheme for two neighboring cells. (B) Time course of *Neurog3* mRNA expression in a ring of nine cells. The different cells stabilize after one, two, or four oscillations. (C) The snapshots of the simulation show *Neurog3* mRNA concentration as blue color intensity for each cell. Time points chosen are 1500, 2500, 3500, 4500, and 5500 min. (D) Time course showing the percentage of *Neurog3*+ cells in the duct for five simulation runs starting with different random number-generator seeds.

other GRNs discussed for patterning by LI, we integrated possibilities for a direct HES1 inhibition on the *Dll1* promoter and a direct negative feedback of *Hes1* onto its own promoter as discussed for neurogenesis (Shimojo et al., 2011) and somitogenesis models (Tiedemann et al., 2012). DLL1 and NOTCH1 are modeled with compartments for the proteins in the cytoplasm and the membrane. *Dll1* mRNAs are modeled for the cytoplasm and the nucleus. As we assume a simplified model excluding oscillatory behavior of *Notch1* expression (see discussion), a description without a separate compartment for the nuclear protein and mRNA is sufficient. The model is intended to simulate mouse development. We use reaction rates from the literature as far as they are known. For D/N signaling, we mostly adopt the rates from our previous simulations (Tiedemann et al., 2012). As NEUROG3 like HES1 is a basic helix-loop-helix (bHLH) protein decaying with a half-life of 20–30 min (Roark et al., 2012), we take over the differential equation system and reaction rates from HES1 with the exception for the promoter structure. We introduced the EMT master control gene *Snail2* into our network as a direct target of NEUROG3 with a long half-life (Gouzi et al., 2011). If a user-defined threshold is surpassed, the cells begin a random walk out of the duct. The program detects the gap and a neighboring cell divides to fill it. We assume NEUROG3+ cells outside of the duct as non-proliferating due to the induction of the cell-cycle inhibitor *Cdkn1* (Miyatsuka et al., 2011). Our simu-

lations do not describe the shutdown of *Neurog3* expression within 24 h in definite endocrine progenitors (Beucher et al., 2012) and their differentiation into hormone producing islet cells, as these processes are outside the scope of the model at this stage of development.

2.3. Simulating noise in the system

Since LI requires small differences in gene expression that are strengthened through D/N interaction and negative feedback (Sprinzak et al., 2010), one has to introduce noise into the simulation, which can be accomplished as follows:

a) Cells are created with start values for each gene product. The addition of random values provides the differences between the cells, upon which LI acts.
b) The daughter cells inherit the concentration values of their mother cells, but turn off transcription during mitosis. We discriminate between regions consisting of one or more than one cell layer. In case of one proliferation layer, the duration of mitosis is randomly Poisson-distributed for which we use methods implemented in the Colt java libraries. If multiple cell layers proliferate, the mitosis duration for newly formed cells does not change but their starting point varies, which means, each daughter cell's mitosis starts at a different normally distributed growth step during proliferation.
c) Instead of ordinary differential equations with 'noisy' initial conditions, molecular noise can be added directly by stochastic terms within the differential equations, which describe fluctuations of chemical-species concentrations around the concentration mean value. We solved this stochastic differential equation system, also known as chemical Langevin equation (Gillespie, 2000), by means of the Euler-Maruyama method, which has been implemented within the open source LibSDE Java library (Schaffter, 2010). The stochastic noise is thereby regulated by a variable (editable on the Java GUI), which effects the generation of the independent Wiener process samples.

2.4. Patterning through D/N in a growing pancreatic duct

Fig. 2 shows the results for a network in which NEUROG3 activates *Dll1* expression and HES1 inhibits *Neurog3* expression. The GRN for two neighboring cells in Fig. 2A shows for convenience the same notation for both the protein and the mRNA. Except for terminal cells, each cell of the growing tube exchanges D/N signals with six neighbors. Fig. 2B shows *Neurog3* expression in the time course for a ring of nine cells. In the simulation time course, up to four oscillations with a period of ~21 h occur before some cells stabilize with maximal and others with minimal expression. Fig. 2C depicts simulation snapshots at five time points, whereby the blue color intensity correlates with *Neurog3* mRNA concentration. If one examines *Neurog3* expression along the whole duct, the characteristic LI-pattern predominates in the older, left part of the duct, whereas in the younger part, *Neurog3*+ cells form patches that come and go. One should notice that this pattern does not form at once but gradually. As can be seen in the provided Movie 1, some cells around few *Neurog3*+ cells transiently express high *Neurog3* levels and eventually calm down to minimal expression. Occasionally, small patches with a LI-pattern come up, only to disappear later. Perhaps, they do not 'fit' properly to the already established hexagonal 1:2 LI-pattern and are 'forced out of the pattern' by the LI of the other cells. Because all initial starting conditions are randomly chosen, this gradual and random establishment of the patterning is probably to be expected in a dynamic system.

2.5. Results for different noise sources

The simulation shown in Fig. 2 and Movie 1 used noise introduced by the transcription stop during M-phase of mitosis. A simulation without shut-off during mitosis but instead addition of a random number in a fixed range (0 to 30) to the protein and mRNA concentrations show a similar patterning (Fig. S1 and Movie 2). A simulation using a Langevin-equation system is shown in Fig. S2 and Movie 3. Due to the added stochastic noise the concentration curves of single cells over time are not smooth anymore. However, the resulting pattern is similar to simulations using initial noise or noise introduced by mitosis.

2.6. Size- and growth-rate effects

For a better visibility, our simulations mostly use a tube architecture with a nine-cell circumference, which might be a bit too large (Pan and Wright, 2011). Simulation snapshots with duct circumferences of five to ten cells are shown in Fig. S3A. With the exception of the smallest circumference, where the periodic boundary condition perpendicular to the growth direction might influence the LI-patterning process, the results for *Neurog3* expression are basically similar. Likewise, halving or doubling the growth rate does not change the system behavior (Fig. S3B).

2.7. Model robustness under parameter variation

Our program is designed for the interactive input of reaction rates and the resulting observation of cellular behavior. This, and the fact that LI patterning appears only gradually after transient expression of *Neurog3* with a variable number of expression peaks/oscillations for each cell, prevents an automatic examination of simulation runs.

First, we varied the reaction rate determining the NICD production as result from the interaction of DLL1 on one cell with NOTCH1 on neighboring cells (trans activation). Stepwise halving the reaction rate from 0.05 to 0.0002 does not change the patterning process and results in stable *Neurog3*+ cells surrounded by negative cells. By halving down to 0.0001, we observe a pattern where many *Neurog3*+ cells have a positive cell as a direct neighbor (Fig. 3). Halving again leads to a breakdown of the process, at least for the observed period, until *Neurog3* is not inhibited anymore by HES1 and shows constant expression. Before this happens, one can observe an inverted LI pattern, i.e. *Hes1* expressing cells surrounded by *Neurog3* expressing cells. However, since the patterning process is stable even under variation of the coupling by more than two orders of magnitude, we consider our model of LI in this regard as robust.

Interestingly, weakening of D/N signaling seems to increase the propensity of the cell system towards synchronization. Moving patches of *Neurog3*+ cells at the beginning of the simulation synchronize into moving stripes. They arise when moving *Neurog3* patches hit the sharp and regular boundary on the left side of the duct and are 'reflected' there. However, this is a boundary effect. When the stripes move to the left, LI leads again to a decay of the sharp borders.

We also varied other parameters and show that progressive weakening of D/N signaling, which results in weakened HES1 expression, or the direct weakening of *Hes1* expression by e.g. faster decay rates, can lead in extreme cases to a propensity for synchronization and further to a constant *Neurog3* expression (see Fig. S4 and Table S3 for a discussion).

Furthermore, we varied the Hill coefficient of *Dll1, Hes1*, and *Neurog3* by changing the default value of 2 to 1, 3, 4, 8, and 16. However, this does not change the general development of oscillations and later LI-patterning in any case (Fig. S5).

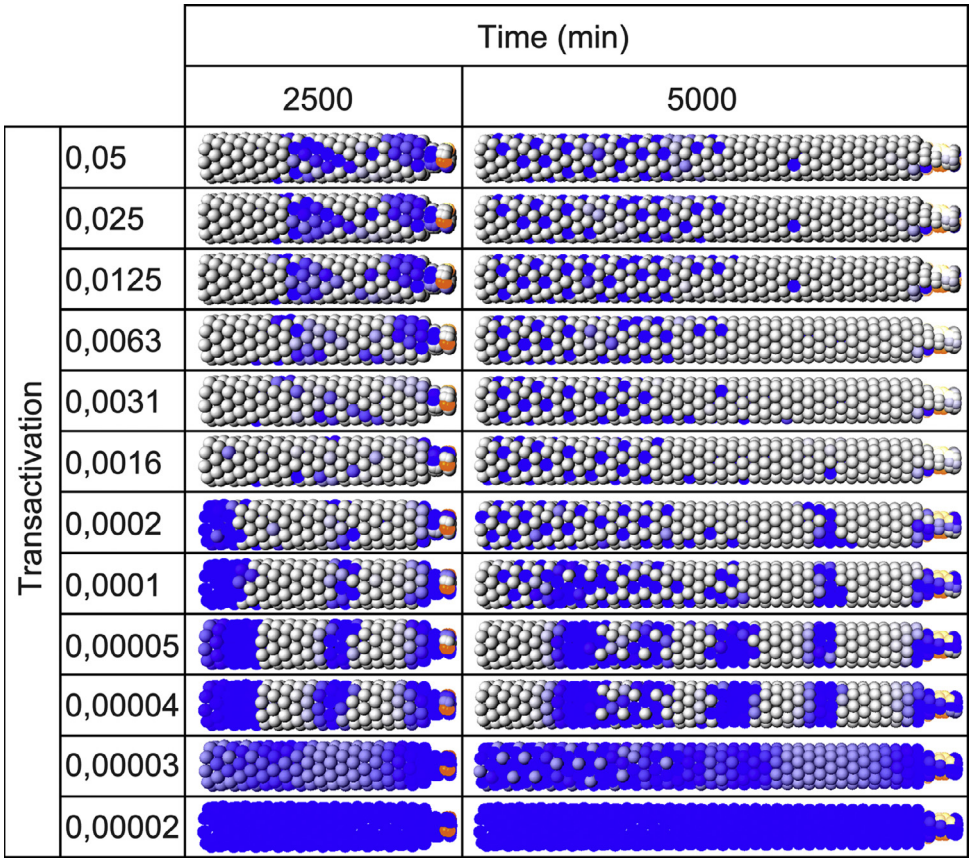

Fig. 3. Variation of the D/N reaction rate. The noise is introduced by a transcription stop during mitosis. Shown are the results for a GRN in which NEUROG3 activates *Dll1* and HES1 inhibits *Neurog3* for different values of D/N reactions rates that lead to the NICD release. Only values of 0.0001 or lower led to a breakdown of the patterning process. The snapshots show *Neurog3* mRNA concentration as blue color intensity for each cell. Time points chosen are 2500 and 5000 min.

2.8. Results for an alternative GRN with additional inhibition of Dll1 *by HES1*

LI is also used as an explanation for the fact that during neurogenesis not all neural progenitors differentiate into neural cells. However, it is assumed that this mechanism acts by a direct inhibitory action of HES1 on *Dll1* and on the *Neurog3* homologous gene *Neurog2* (Shimojo et al., 2011). We therefore performed simulations with a corresponding GRN for *Dll1* regulation (Fig. 4A) but without a Hes1 negative feedback onto itself, which may play an important role in oscillatory gene expression during neurogenesis. Also in this case, LI leads to a stabilized pattern of *Neurog3*+ cells after oscillatory expression (Fig. 4C and Movie 4). However, with around 13 h the oscillation period is shorter than in the above-described standard model (Fig. 2), which is to be expected, since the loop Hes1 – Dll1 – NICD – Hes1 is shorter and the negative feedback along this loop therefore acts after a shorter delay.

2.9. Results for an alternative GRN (similar to somitogenesis)

Inspired by our efforts on modeling somitogenesis, where we postulated a GRN with a negative feedback of HES7 onto *Dll1* expression (Tiedemann et al., 2012), we also examined a network in which HES1 inhibits *Dll1* and *Neurog3* expression, but without a positive feedback of NEUROG3 on *Dll1* (Fig. 5A). Again, the LI-pattern forms with similar dynamics (Fig. 5B, C and Movie 5) as seen for the GRN examined above.

2.10. Adding negative feedback of Hes1 onto itself to the standard GRN

In neurogenesis, *Hes1, Neurog2*, and other genes show oscillatory gene expression (Shimojo et al., 2008) with shorter periods than in our models, namely 2–3 h compared to 21 or 13 h, respectively. Said oscillations are of the ultradian type and presumably caused by a negative feedback of HES1 onto its own promoter in addition to the short decay rates of *Hes1* mRNA and its protein of about 20 min (Hirata et al., 2002). We added such a negative HES1 feedback to our standard model:

Oscillatory case. A negative feedback in the *Hes1* promoter as modeled for somitogenesis (Fig. 6A) results in ultradian *Hes1* oscillations that induce corresponding *Neurog3* oscillations in antiphase, because HES1 suppresses *Neurog3*. Consequently, these oscillations do not die down (Fig. 6B) and prevent the emergence of a stable pattern of *Neurog3*+ cells (Fig. 6C and Movie 6).

Non-oscillatory case. The parameter space, which allows oscillation in the negative-feedback oscillator *Hes1*, was already determined by our efforts on somitogenesis (Tiedemann et al., 2012, 2007). If one chooses a transcription or translation rate that does not allow *Hes1* oscillation (e.g. by halving the *Hes1* transcription rate), the pattern formation is still suppressed. Both *Hes1* and *Neurog3* show a uniform expression (Fig. S6). Probably, the negative feedback is still operating, but instead of generating oscillations it suppresses all cell-to-cell expression differences. Since small expression differences between cells are needed for LI to amplify these distinctions, the pattern cannot be established.

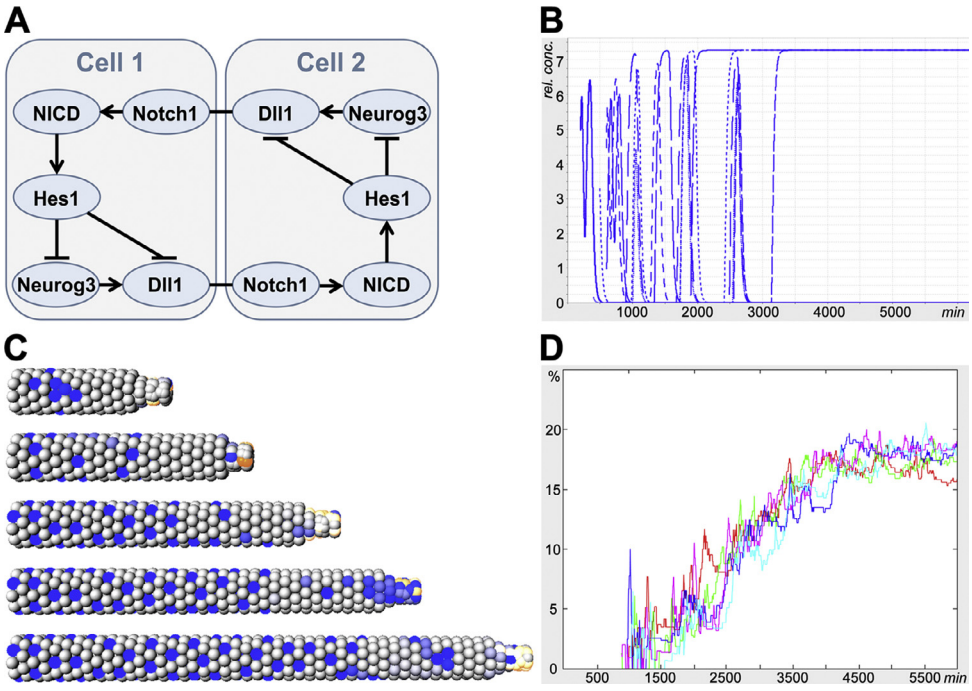

Fig. 4. Simulation result for a GRN adapted from neurogenesis in which NEUROG3 activates *Dll1* and HES1 inhibits not only *Neurog3* but also *Dll1*. The noise is introduced by a transcription stop during mitosis and standard parameters were used (Table S1). The Hill functions and -thresholds are described in Table S2. (A) Reaction scheme for two neighboring cells. (B) Time course of *Neurog3* mRNA expression in a ring of nine cells. (C) The snapshots show *Neurog3* mRNA concentration as blue color intensity for each cell. Time points chosen are 1500, 2500, 3500, 4500, and 5500 min. (D) Time course showing the percentage of *Neurog3*+ cells in the duct for five simulation runs starting with different random number-generator seeds.

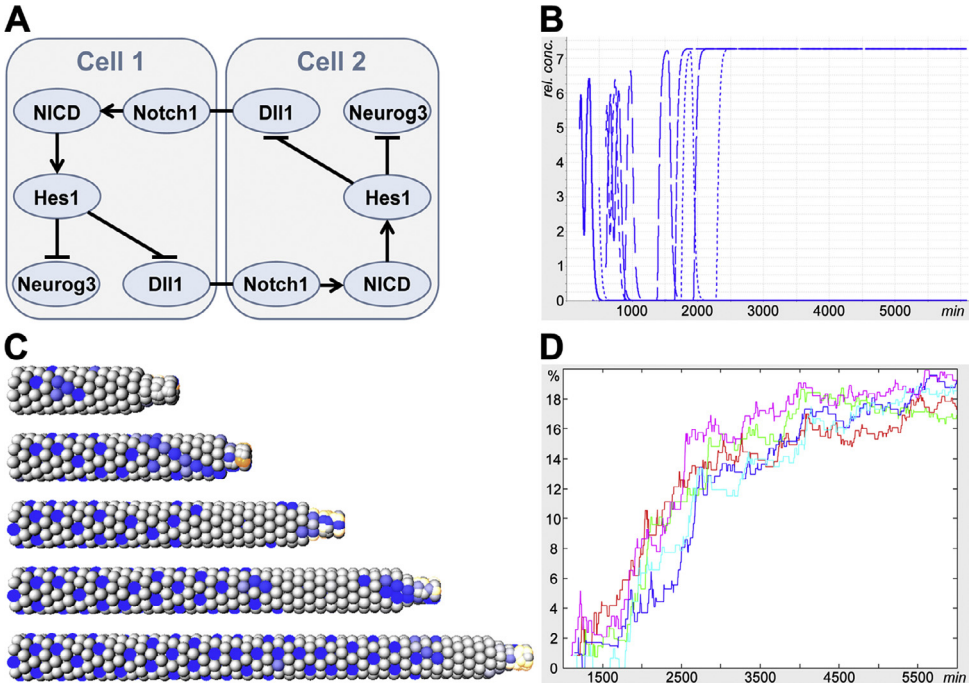

Fig. 5. Simulation result for a GRN adapted from somitogenesis in which HES1 inhibits *Neurog3* and *Dll1*, but without a positive feedback of NEUROG3 on *Dll1*. The noise is introduced by a transcription stop during mitosis and standard parameters were used (Table S1). The Hill functions and -thresholds are described in Table S2. (A) Reaction scheme for two neighboring cells. (B) Time course of *Neurog3* mRNA expression in a ring of nine cells. (C) The snapshots show *Neurog3* mRNA concentration as blue color intensity for each cell. Time points chosen are 1500, 2500, 3500, 4500, and 5500 min. (D) Time course showing the percentage of *Neurog3*+ cells in the duct for five simulation runs starting with different random number-generator seeds.

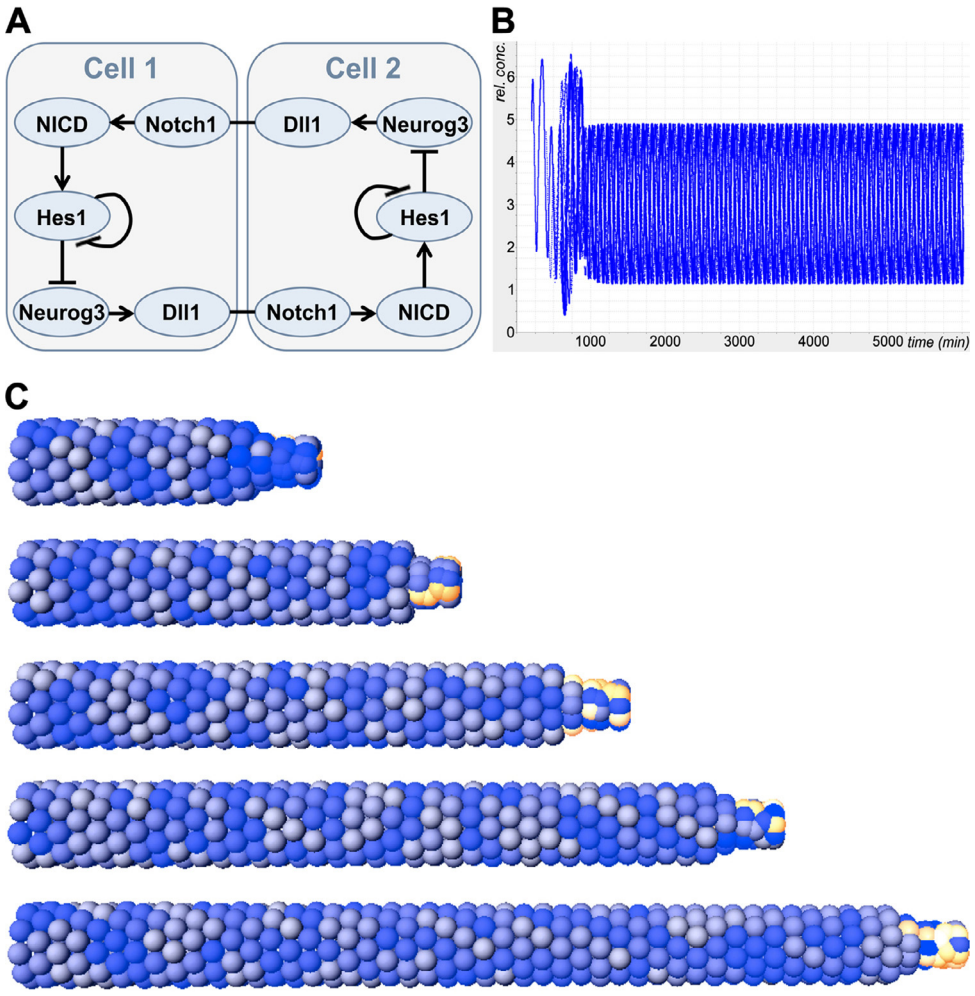

Fig. 6. Adding negative feedback of Hes1 onto itself. Shown are the results for a GRN in which NEUROG activates *Dll1* and HES1 inhibits *Neurog3* and itself. The noise is introduced by a transcription stop during mitosis and standard parameters were used (Table S1). The Hill functions and -thresholds are described in Table S2. (A) Reaction scheme for two neighboring cells. (B) Time course of *Neurog3* mRNA expression in a ring of nine cells. (C) The snapshots show *Neurog3* mRNA concentration as blue color intensity for each cell. Time points chosen are 1500, 2500, 3500, 4500, and 5500 min.

Progressive weakening of the Hes1 negative feedback onto itself. Instead of simulating models where Hes1 negative feedback is either included or excluded, one can think of mechanisms that weaken the negative feedback of HES1 on its promoter but not HES1 binding to the promoters of *Neurog3* or *Dll1* (Bai et al., 2007). We therefore progressively increased the Hill threshold in the inhibiting Hill-function of the *Hes1* promoter. By using a 16-fold higher threshold, we observed a completely new system behavior. At first, the ultradian oscillations prevent a stable pattern. But after about 40 h, the first permanently non-oscillating *Neurog3*+ cells show up, which later form the usual 1:2 pattern. However, these stable *Neurog3*+ cells are still surrounded by oscillating cells (Fig. 7 and Movie 7).

2.11. Coupling an FGF10 gradient to the Hes1 mRNA decay

As another possibility to arrest negative-feedback *Hes1* oscillations we consider the influence of an FGF10 gradient along the pancreatic duct, where maximum *Fgf10* expression is at and stops outside the growth zone. Since we do not model the neighboring mesenchymal cells, one has to note that the gradient is not generated by diffusion but travels along the growing tip, which is rather unrealistic. As described for somitogenesis (Tiedemann et al., 2007), we assume a slow *Fgf10* mRNA decay and couple the *Hes1* mRNA decay to the FGF10 gradient. Thus, the *Hes1* mRNA decay rate slowly decreases to zero for cells outside of the growth zone, which leads to a *Hes1*-oscillation stop. However, the ratio of *Neurog3*+ to negative cells is thereby clearly lower than one third and does not reflect the *in vivo* situation (Bankaitis et al., 2015), and the cells express *Neurog3* only weakly (Fig. 8), wherefore it is questionable whether this mechanism should be considered as realistic.

2.12. Introducing Snail2 and cell delamination

In Movie 8 we show a simulation when *Snail2* is activated downstream of NEUROG3, to demonstrate delamination of cells from the duct when a certain threshold of SNAIL2 is exceeded. A delaminating *Neurog3*+ cell is replaced by a neighboring *Neurog3*– cell, which proliferates to fill the gap. After a while, the new cell in the center expresses *Neurog3* again. How long it takes to delaminate again depends on the SNAIL threshold.

We also tested the behavior of the system when delamination is active for different GRNs and show the results in Fig. S7. The non-standard models show the full LI pattern earlier. Hence, the pattern of *Neurog3*+ cells in these cases is more similar to simu-

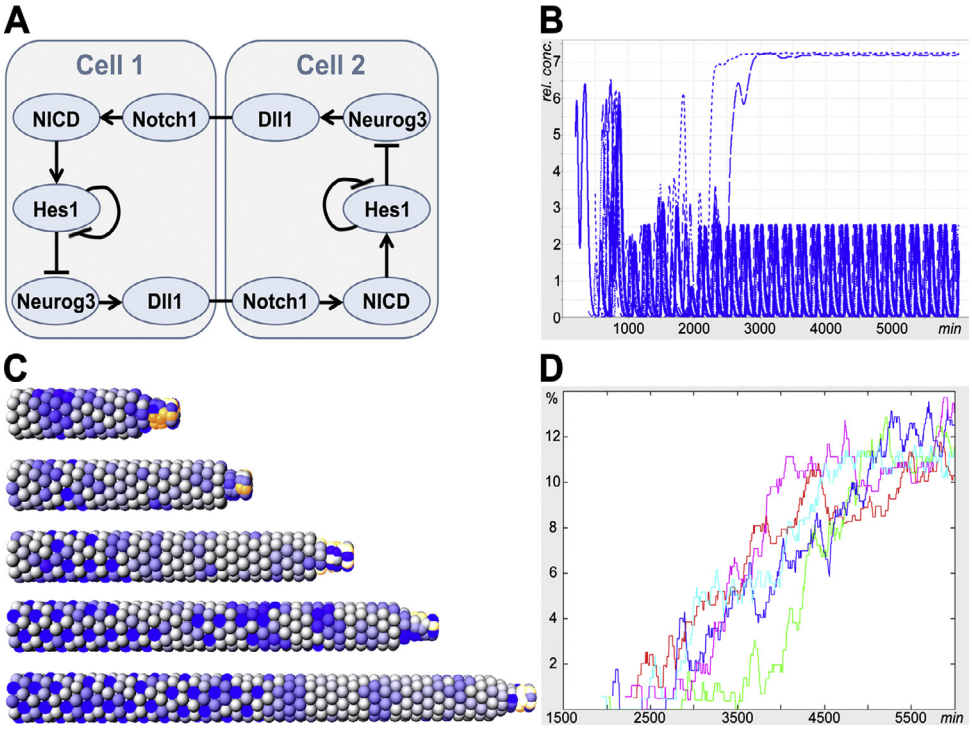

Fig. 7. Weakened Hes1-negative feedback onto itself. Shown are the results for a GRN in which NEUROG activates *Dll1* and HES1 inhibits *Neurog3* and itself. Standard parameters were used (Table S1). The Hill functions and -thresholds are described in Table S2. A Hill threshold of 16 weakens the negative feedback of HES1 onto its own promoter. The noise is introduced by a transcription stop during mitosis. (A) Reaction scheme for two neighboring cells. (B) Time course of *Neurog3* mRNA expression in a ring of nine cells. Seven of these cells show ultradian oscillations until the end of the simulation, while two stabilize *Neurog3* expression at higher concentration, i.e. become determined in an LI pattern. (C) The snapshots show *Neurog3* mRNA concentration as blue color intensity for each cell. Time points chosen are 1500, 2500, 3500, 4500, and 5500 min. (D) Time course showing the percentage of *Neurog3*+ cells in the duct for five simulation runs starting with different random number-generator seeds.

lations without delamination. However, as we do not have enough information on the biological control of delamination *in vivo* it is premature to draw any conclusions from our delamination modeling.

3. Discussion

3.1. Issues in pancreas development

Several questions regarding pancreas development are still under discussion. For example, which signal-transduction pathway in which time course determines the proportion of *Neurog3*+ endocrine precursor cells in the pancreatic duct during secondary transition (Afelik and Jensen, 2013)? Does *Hes1* oscillate during pancreas development as in neurogenesis, where *Neurog2* and D/N-mediated LI regulate the generation of neural progenitors (Imayoshi and Kageyama, 2014)? If not, why is then dynamic behavior of *Hes1* different although the GRNs are so similar?

Here, we address these questions and summarize our modeling efforts as follows: (i) several different GRNs can explain the generation of stable *Neurog3*+ cells; (ii) oscillatory gene expression can precede pattern formation through LI; (iii) the typical LI-pattern (one cell with high and stable *Neurog3* expression surrounded by *Neurog3* negative cells) builds not at once, but gradually; (iv) not the resulting pattern but the length of the oscillatory phase depends on the delay in the negative feedback loop; (v) when sufficiently weakened, the Hes1 negative self-feedback allows or even promotes pattern formation. In this case, the cells surrounding *Neurog3*+ cells are not completely devoid of *Neurog3*, but show distinct lower and rapidly oscillating *Neurog3* expression.

3.2. Simplifications in modeling gene interactions

To keep the model complexity within reasonable limits we have made some simplifications:

- For simulating D/N signaling, we consider only DLL1 as ligand and NOTCH1 as receptor, although increasingly more information on the pathway and its function in pancreas development is available (for reviews see (Afelik and Jensen, 2013; Pan and Wright, 2011)). For example, we neglected JAGGED1, which seems to be required for proper duct formation and act as a competitive Notch inhibitor during primary transition (Golson et al., 2009a, b). Contrary to *Dll1*, we assume that the *Notch1* expression is static, although it was recently shown to be dynamic on both the mRNA and protein level during somitogenesis (Bone et al., 2014). However, compared to DLL1, the NOTCH1 oscillation amplitude was smaller, therefore we keep this simplification for our exploratory model.
- Although NEUROG2 and presumably NEUROG3 bind as a hetero-dimer with the E-box binding protein TCF3 to the *Dll1* promoter (Imayoshi and Kageyama, 2014), in our model NEUROG3 activates *Dll1* directly.
- Because in D/N signaling the NICD acts in concert with MAML1 and RBPJ in a higher-order transcription complex (Nam et al., 2007), we specified NICD binding as a dimer to the *Hes1* promoter. However, if one wants to simulate the differentiation of the *Ptf1a* expressing tip- into acinar cells, RBPJ as part of the PTF1A complex and its replacement by RBPJL, which is induced by this complex, has to be included (Masui et al., 2007). The RBPJL-PTF1A complex then induces the nuclear receptor gene *Nr5a2*, which is required for proper acinar differentiation (Hale et al., 2014).

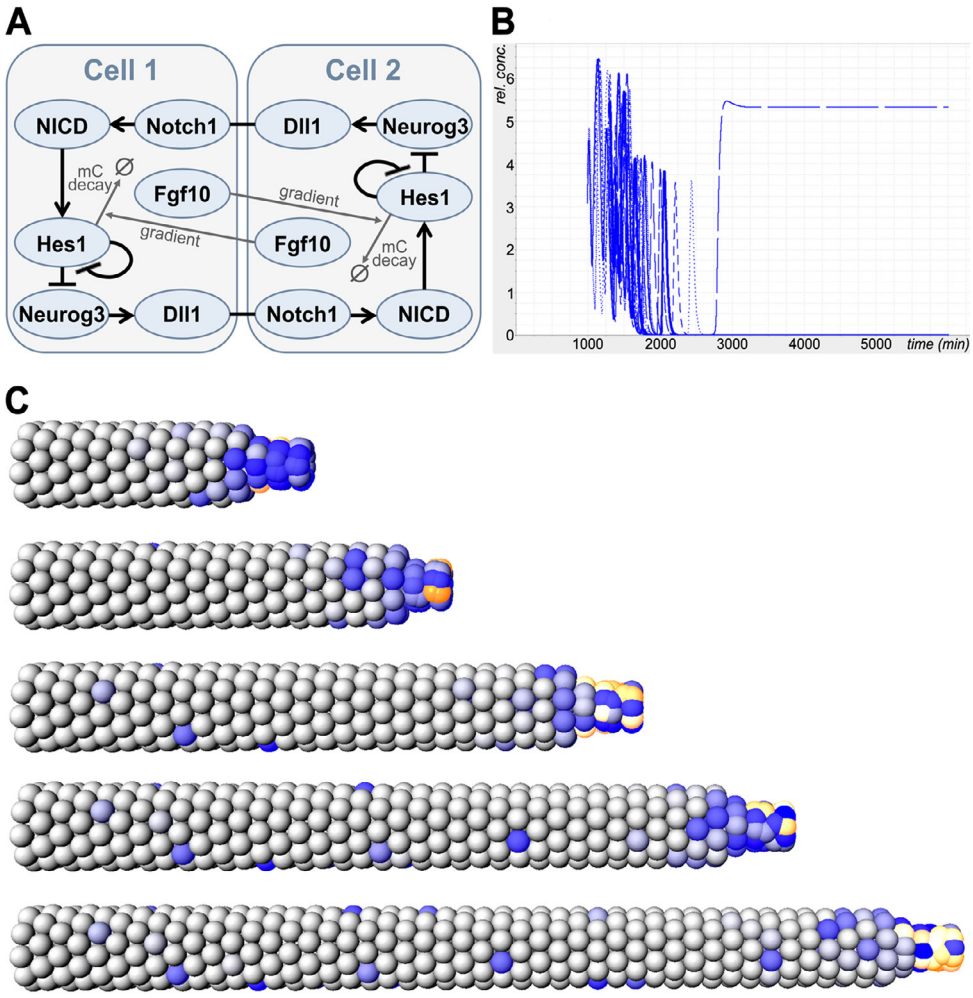

Fig. 8. Hes1 negative feedback onto itself influenced by FGF10 in the standard GRN, in which NEUROG3 activates *Dll1* and HES1 inhibits *Neurog3* and itself. *Fgf10* is expressed in the growth zone and decays slowly, which generates an FGF10 gradient along the growing duct that diminishes the *Hes1* mRNA decay proportionally. The noise is introduced by a transcription stop during mitosis. (A) Reaction scheme for two neighboring cells. (B) Time course of *Neurog3* mRNA expression in a ring of nine cells. (C) The snapshots show *Neurog3* mRNA concentration as blue color intensity for each cell. Time points chosen are 1500, 2500, 3500, 4500, and 5500 min.

- While for somitogenesis simulations we had a clear picture how Wnt3a signaling induces *Dll1* and *Notch1* in the presomitic mesoderm (Tiedemann et al., 2012), here we lack information on such an influence. Although Wnt7b and Fgf10 operate in pancreas development, elimination of *Wnt7b* did not abolish the patterning of *Neurog3*+ cells (Afelik et al., 2015). Moreover, modeling the impact of Wnt7b and Fgf10 signaling on a network of ducts growing into the mesenchyme is not simple. We also neglected binding of PTF1A on the *Dll1* promoter (Ahnfelt-Ronne et al., 2012). Instead, we used constant induction of *Dll1* and *Notch1* along the growing duct.
- As mechanism for weakening the Hes1 negative feedback onto its own promoter, binding of ID (inhibitor of DNA-binding) proteins was proposed (Bai et al., 2007), which might also interact with the NEUROG3-binding partner TCF3 (Imayoshi and Kageyama, 2014). However, we refrained from including an *Id* gene into our GRN and simulated instead a diminished action of HES1 onto its own promoter by increasing the Hill threshold for HES1 action in the function describing the *Hes1* promoter.
- Assuming an FGF10 gradient along the duct in our model does not reflect the geometric complexities of a growing pancreas during secondary transition. Instead it serves as a possible mechanism how a stable pattern of NEUROG3+ cells in the duct can be generated. Certainly, the low *Neurog3*+ ratio by this simplified modeling seems to be unrealistic when compared to the actual numbers observed during the secondary transition of pancreas development (Bankaitis et al., 2015).
- A mesenchymal FGF10 signaling to the duct might exert additional effects like a phosphorylation of downstream targets. In neurogenesis, for example, phosphorylated NEUROG2 binds to the *Dll1* but not to the *Neurod1* promoter, whereas non-phosphorylated NEUROG2 binds to both promoters equally (Imayoshi and Kageyama, 2014).

3.3. Other genes excluded from the simulation

- *Hes6*, induced by NEUROD1 (Hoffman et al., 2008), inhibits *Hes1* directly. Hence, a *Neurog3*+ cell, which induces *Neurod1*, could become inert to D/N signaling when NEUROD1 is expressed long enough. This could be a mechanism to ensure the stable *Neurog3* and *Neurod1* expression after *Neurog3*+ cells left the epithelium and migrated into the mesenchyme where they are possibly exposed to NOTCH3 signaling. However, *Hes6* was only detected at E14.5 in the duct epithelium (Hoffman et al., 2008).
- *Sox9*. Shih et al. (2012) suggested a GRN in which graded Notch signaling regulates the generation of both the ductal and the endocrine cell fates by Notch-activity dependent induction of

the *Neurog3* repressor HES1 and the *Neurog3* activator SOX9. However, we did not completely include this in our GRN.

- *Mfng* and *Lfng*. In mammalian systems, Lunatic fringe (LFNG), Manic fringe (MFNG) and Radical fringe (RFNG) are known to modify Notch receptors by O-fucosylation (Shao et al., 2003). While RFNG is not expressed in the pancreas, LFNG is found only in ductal tips and *Mfng* seems to be dispensable for pancreas development (Svensson et al., 2009). We therefore do not take modification of NOTCH by LFNG into consideration.

3.4. Result interpretation and comparison to biological experiments

Our model is a first step towards a more comprehensive understanding of pancreas development. We neglected several genes downstream or upstream of NEUROG3, for which more or less detailed information already exists (for reviews see (Cano et al., 2014; Shih et al., 2013) and references therein). Nevertheless, as long as mutual inhibition between neighboring cells is guaranteed, our simulations suggest that patterning by LI is independent from the GRN architecture. With appropriate weakening even the integration of a Hes1 negative feedback is possible. Summing up, our results argue for a general mechanism in terms of a 'dynamical patterning module' (Newman and Bhat, 2009) of oscillatory gene expression and D/N-mediated LI in several developmental processes such as neuronal differentiation (Shimojo et al., 2011), intestinal lineage specification (Philpott and Winton, 2014) and the generation of pancreatic endocrine progenitors.

The integration of a weakened Hes1 negative feedback onto itself results in a new spatio-temporal pattern, coupling D/N-mediated LI with oscillating cells surrounding stable *Neurog3*+ cells. For neurogenesis, Bai et al. (2007) identified ID proteins that act on Hes1 negative-feedback autoregulation without affecting the binding to other target genes . A similar mechanism might occur during the secondary transition of pancreatogenesis, where BMP4 induces expression of *Id2* in pancreatic epithelia (Hua et al., 2006). In lung development, Wnt7b signaling induces *Bmp4* and *Id2* in growing epithelial tips (Rajagopal et al., 2008). However, the genetic deletion of *Wnt7b* during pancreatogenesis does not influence the differentiation of endocrine progenitors (Afelik et al., 2015).

Our simulations should be understood as toy models showing the temporal and spatial expression of *Neurog3* as depicted schematically and reviewed by Pan and Wright (2011): a patchy and transient *Neurog3* expression followed by a gradual appearance of the characteristic LI-pattern. The coupling of growth and oscillations has the effect that the duration of the oscillatory phase determines the distribution of endocrine progenitors. The longer the oscillatory phase lasts until stabilization, the more *Neurog3*+ cells are located in the inner (e.g. developmentally older) parts of the duct network. Recently, Bankaitis et al. (2015) showed that in the inner part of the growing pancreas – characterized as 'plexus' by the authors – the ratio of *Neurog3* to *Sox9* expressing duct cells is approximately 1:3, while in the outer part, characterized by ductal formation and growth, the ratio is much lower (ca. 1:10). However, too many unknown processes regarding plexus epithelialization and remodeling prevent us from demonstrating the full complexity of pancreas formation, so a direct comparison to our simplified model is difficult. Nevertheless, in our simulations the order of magnitude of the ratio of *Neurog3*+ to negative cells seems to agree with the findings of Bankaitis et al. (2015). So, contrary to a recently published model on early pancreatic patterning by de Back et al. (2013), we see no need to introduce a hypothetical lateral-stabilization mechanism in parallel to LI to explain the number and scattered distribution of *Neurog3*+ cells, because the sparse occurrence of these cells in our model depends on which part of the growing duct, developmentally older or younger, is observed. An advantage of our model with negative HES1-feedback onto its own promoter could be seen in the occurrence of many cells expressing low (weakly and fast oscillating) levels of *Neurog3*, instead of many cells expressing no *Neurog3* at all, like in the other models.

3.5. Outlook

Time- and single-cell resolved observations of pancreatogenesis *in vitro* and *in vivo* might help to decide between our model, which incorporates the standard LI-mechanism plus growth and oscillatory gene expression, and a model postulating additional lateral stabilization (de Back et al., 2013). For example, real-time imaging of different reporter mice for potentially oscillatory genes could be combined with conditional deletion in a temporal manner. In this context, recent results from Shimojo et al. (2016) are of particular interest, which showed oscillating DLL1 expression in somitogenesis and neurogenesis . Such experiments might also clarify whether a HES1 negative feedback onto its own promoter is active in pancreatogenesis and influenced by *Id* and *Bmp* genes. Also the action of PTFA1 on *Dll1* (Ahnfelt-Ronne et al., 2012) could be integrated into the GRN of D/N, Hes1 and Neurog3 for further simulations. Unsatisfying is the knowledge gap how the pancreatic mesenchyme signals through FGF10 and WTN7B to the duct epithelium and whether there is reverse signaling between them as described for lung development (Volckaert and De Langhe, 2015). Recently, Willmann et al. (2016) identified many novel regulators that are differentially expressed in epithelial and mesenchymal compartments of the developing pancreas and which ultimately should be included in a better simulation of progenitor determination.

At present, we phenomenologically modeled the ablation of stable *Neurog3*+ endocrine precursors from the duct. An extended GRN could therefore contain *Snail2* as well as Ephrin-family members to analyze the EMT (Villasenor et al., 2012), which then enables further differentiation.

The fact that our 'cells' are incompressible prevented us from exploring all possible scenarios for cell proliferation prior to patterning. More realistic cell mechanics, which include movement and adhesion, should be a future goal. Likewise, the mutual influence of D/N signaling and the cell cycle should be included. It remains to be seen whether these shortcomings of our model can affect the occurrence of the predicted long-period oscillations.

3.6. Conclusion

The results of our modeling efforts can be summarized as follows:

- The typical salt-and-pepper pattern does not form at once but with a substantial delay and initially only a few cells with stable *Neurog3* expression depending on the GRN topology.
- Instead, transient patches of *Neurog3*+ cells move along the duct and disappear because only after a transient oscillatory phase the cells settle in a stable LI pattern. So, there is no need to postulate other processes in addition to D/N signaling.
- Including a Hes1 negative self-feedback as assumed to be operating in neurogenesis allows the coexistence of stably *Neurog3* expressing cells surrounded by oscillating *Neurog3* expressing cells with a smaller amplitude so long as the Hes1 self-feedback is sufficiently weakened.
- Hence, differences between D/N signaling in neurogenesis and pancreatogenesis may be not grounded on different GRN topologies but on different post-transcriptional regulation of HES1 onto its own promoter.

Our efforts demonstrate that oscillatory expression of Notch signaling components and LI during secondary transition of pan-

creatogenesis seem to be not mutually exclusive to generate *Neurog3*+ endocrine precursors. We are convinced that the most important features of a realistic model are growth and the possibility of oscillatory gene expression, since growth can translate temporally into spatial gene-expression differences and oscillatory expression seems to be a general mechanism to keep progenitor cells poised before lineage decision (Kobayashi et al., 2009).

In summary, modeling aspects of pancreatogenesis *in silico* might help to design the right *in vivo* and *in vitro* experiments. The results will then contribute to develop new differentiation protocols for functional beta cells that can be used for replacement therapies.

4. Methodology

4.1. General features

We model gene expression using the same methodology as described in our previous work (Tiedemann et al., 2007). This gene- and cell-based simulation program solves differential equations describing a gene regulatory network and displays the concentration of a selected gene product by color intensity in each cell (virtual *in situ* staining).

In the following, Hill functions of the form $R_h(x) = H_R^h/(H_R^h + x^h)$ are used to describe an inhibiting influence of a protein/transcription factor on gene expression. The Hill-coefficient h is a measure for the cooperativity of repressor binding to the promoter. H_R is the threshold concentration of x, where inhibition halves gene expression, while H_A is the threshold determining half-activation. To simulate activating gene action we use Hill functions of the form $A_h(x) = x^h/(H_A^h + x^h)$. If transcription factors bind as homo-dimers, the Hill-coefficient is 2.

To describe oscillating gene expressions, caused by a delay between gene expression and a negative feedback onto itself, essentially two mathematical formalisms exist. Oscillations can be modeled either with direct introduction of delayed arguments into differential equations specifying the time used for gene transcription and translation into protein, which results in a so-called delay-differential equation system (e.g. see Lewis, 2003; Monk, 2003), or with a transport-equations chain between different cell compartments. We decided for the compartment model because with delay models, which require more computer memory and are mathematically more difficult, we did not find a solution to combine the delays with proliferation and the introduction of noise to make the cells slightly different. If one wants to minimize the number of transport equations/compartments and use of reasonably small Hill coefficients, one has to introduce the saturated protein-decay term in the nucleus as additional non-linearity (Murray, 2002). We have two compartments for mRNA in the nucleus and in the cytoplasm (mN and mC) and three possible compartments for proteins: in the nucleus, the cytoplasm, and the membrane (designated PN, pC, and pM).

The equations below describe the GRN generating *Neurog3* patterning. Mostly, we explicitly write down gene indices on the variables written on the right side of the equations only when they refer to other genes. Otherwise they are suppressed. Decay-rate units are in min^{-1}, concentration values are in arbitrary units. The transcription and translation rates are designated as k and K, respectively. The export rates start with the letter 'e', the degradation rates with 'd', except the assumed non-linear protein degradation in the nucleus that is characterized by G and F.

Hes1

$$\frac{d(pC_{Hes1}(t))}{dt} = K \cdot mC(t) - dpC \cdot pC(t) - epC \cdot pC(t) + epN \cdot pN(t)$$

$$\frac{d(pN_{Hes1}(t))}{dt} = epC \cdot pC(t) - \frac{G \cdot pN(t)}{F + pN(t)} - epN \cdot pN(t)$$

$$\frac{d(mC_{Hes1}(t))}{dt} = emN \cdot mN(t) - dmC \cdot mC(t)$$

$$\frac{d(mN_{Hes1}(t))}{dt} = k \cdot H_h(t) - dmN \cdot mN(t) + emN \cdot mN(t)$$

The Hill function $H_h = R_3(pN_{Hes1}) \cdot A_2(pN_{NICD})$ with $H_A = 4.5$ describes the control of Hes1 transcription by the NICD. The inhibitory Hill function $R_3(pN_{Hes1})$ with $H_R = 1.0$ or higher is used only for the model with an additional HES1-negative feedback onto its own promoter, otherwise 1 replaces it. As *Hes1* is a target of D/N signaling, the NICD acts as transcriptional co-factor on the *Hes1* promoter. Two complexes comprising NICD, MAML1 and CSL bind as dimer to the *Hes1* promoter (Nam et al., 2007). Therefore, we use a Hill-coefficient of 2 in the function describing the NICD effect. For the decay rates of Hes1 protein and mRNA we use the values already described (Hirata et al., 2002). All production-, decay- and export rates (Table S1) are adopted from our previous publication on somitogenesis (Tiedemann et al., 2012).

Neurog3

$$\frac{d\left(pC_{Neurog3}(t)\right)}{dt} = K \cdot mC(t) - dpC \cdot pC(t) - epC \cdot pC(t) + epN \cdot pN(t)$$

$$\frac{d\left(pN_{Neurog3}(t)\right)}{dt} = epC \cdot pC(t) - \frac{G \cdot pN(t)}{F + pN(t)} - epN \cdot pN(t)$$

$$\frac{d\left(mC_{Neurog3}(t)\right)}{dt} = emN \cdot mN(t) - dmC \cdot mC(t)$$

$$\frac{d\left(mN_{Neurog3}(t)\right)}{dt} = k \cdot H_h(t) - dmN \cdot mN(t) - emN \cdot mN(t)$$

Since HES1 suppresses *Neurog3*, we chose $H_h = R_2(pN_{Hes1})$ with $H_R = 1.0$. Since NEUROG3 as a bHLH transcription factor has a half-life of 20–30 min like HES1, we use for *Neurog3* the same decay and production rates as for *Hes1*. For a complete set of parameters see Table S1.

NICD

After binding of DLL1 to NOTCH1, the receptor is cleaved by proteases and the NICD is transported from the cytoplasm into the nucleus (Rida et al., 2004).

$$\frac{d(pC_{NICD}(t))}{dt} = r_{DN} \cdot \overline{pM_{Dll1}}(t) \cdot pM_{Notch1}(t) - dpC \cdot pC(t) - epC \cdot pC(t) + epN \cdot pN(t)$$

$$\frac{d(pN_{NICD}(t))}{dt} = epC \cdot pC(t) - \frac{G \cdot pN(t)}{F + pN(t)} - epN \cdot pN(t)$$

$$\overline{pM_{Dll1}}(t) = \frac{1}{n} \cdot \sum^{n} pM_{Dll1}(t), \quad n = number\ of\ neighbors$$

Here, $r_{DN} = 0.05$ specifies the reaction rate between the NOTCH1 receptors and the DLL1 ligands on n neighboring cells. pM_{Notch1} denotes the NOTCH and pM_{Dll1} the DLL1 membrane-protein concentration, respectively. $epC = 0.12$ and $epN = 0.6$ constitute the export rates for the NICD from the cytoplasm to the nucleus and vice versa, and $dpC = 0.2$ the cytoplasmic NICD-decay rate. The rates describing the nuclear decay are $F = 5.0$ and $G = 5.0$. We assume an active transport of the transcription co-factor NICD into the nucleus. So we chose its import rate to the nucleus larger as the export rate (Table S1).

Dll1

Dll1 expression is dynamic in the presomitic mesoderm (Maruhashi et al., 2005) and during neurogenesis (Shimojo et al., 2011). We use two equations for Dll1 mRNA and protein, each in the nucleus and the cytoplasm, because mathematics for negative-feedback systems shows that usage of a transport-equation system

with at least three equations is necessary for the occurrence of an oscillatory behavior (Murray, 2002).

$$\frac{d(pM_{Dll1}(t))}{dt} = epC \cdot pC(t) - epM \cdot pM(t) - dpM \cdot pM(t) - r_{DN} \cdot \overline{pM_{Notch1}}(t) \cdot pM(t) - r_{DNcis} \cdot pM_{Notch1}(t) \cdot pM(t)$$

$$\frac{d(pC_{Dll1}(t))}{dt} = K \cdot mC(t) - dpC \cdot pC(t) - epC \cdot pC(t) + epM \cdot pM(t) - r_{DNcis} \cdot pC_{Notch1}(t) \cdot pC(t)$$

$$\frac{d(mC_{Dll1}(t))}{dt} = emN \cdot mN(t) - dmC \cdot mC(t)$$

$$\frac{d(mN_{Dll1}(t))}{dt} = k \cdot H_h(t) - dmN \cdot mN(t) - emN \cdot mN(t)$$

$$\overline{pM_{\mathrm{Notch1}}}(t) = \frac{1}{n} \cdot \sum^{n} pM_{\mathrm{Notch1}}(t), \quad n = number\ of\ neighbors$$

In our standard model NEUROG3 activates *Dll1*, wherefore we set $H_h = A_2(pN_{Neurog3})$. In the alternative models, where HES1 suppresses *Neurog3*, we set $H_h = R_2(pN_{Hes1})$. The rate constants are set as in our previous publication (Tiedemann et al., 2012) except $dmC{:}K = 1.5$, $dpC = 0.09$, $epC = 0.1$, $epM = 0.1$, $dpM = 0.0$, $dmC = 0.006$, $emN = 0.09$, $dmN = 0.001$ and $k = 1.25$ (Table S1).

Notch1

We assume Notch1 expression to be static. So we simplify the description by using one simple equation for the mRNA concentration without differentiating between the nucleus and the cytoplasm.

$$\frac{d(pM_{\mathrm{Notch1}}(t))}{dt} = epC \cdot pC(t) - epM \cdot pM(t) - dpM \cdot pM(t) - r_{DNcis} \cdot pM_{Dll1}(t) \cdot pM(t) - r_{DN} \cdot \overline{pM_{Dll1}}(t) \cdot pM(t)$$

$$\frac{d(pC_{\mathrm{Notch1}}(t))}{dt} = K \cdot m(t) - dpC \cdot pC(t) - epC \cdot pC(t) + epM \cdot pM(t) - r_{DNcis} \cdot pC_{Dll1}(t) \cdot pC(t)$$

$$\frac{d(m_{\mathrm{Notch1}}(t))}{dt} = k - dm \cdot m(t)$$

$$\overline{pM_{Dll1}}(t) = \frac{1}{n} \cdot \sum^{n} pM_{Dll1}(t), \quad n = \ number\ of\ neighbors$$

The values $K = 1.5$, $dpC = 0.2$, $epC = 0.1$, $epM = 0.0$, $dpM = 0.1$, $dm = 0.02$ and $k = 0.5$ are used for the rate constants (Table S1).

Data accessibility

Our simulation program can be downloaded at http://www.helmholtz-muenchen.de/fileadmin/IEG/ZIP/downloads/simulation15/SIM15.zip. A short manual explaining the graphical user interface is provided in the supplemental information file.

Competing interests

We have no competing interests.

Authors' contributions

HBT, GKHP and MHdA conceived and designed the research. HBT and ES performed the research. ES contributed analytical tools. HBT, ES, JB, GKHP and MHdA analyzed the data. HBT, GKHP, JB and MHdA wrote the manuscript.

Funding

This study was supported in part by a grant from the German Federal Ministry of Education and Research (BMBF) to the German Center of Diabetes Research (DZD). The funding source had no involvement in study design, analysis, data interpretation, writing of the report, and decision to submit the article for publication.

Supplementary materials

Supplementary material associated with this article can be found, in the online version, at doi:10.1016/j.jtbi.2017.06.006.

References

Afelik, S., Jensen, J., 2013. In: Notch Signaling in the Pancreas: Patterning and Cell Fate Specification, 2. Wiley Interdiscip Rev Dev Biol, pp. 531–544. doi:10.1002/wdev.99.

Afelik, S., Pool, B., Schmerr, M., Penton, C., Jensen, J., 2015. Wnt7b is required for epithelial progenitor growth and operates during epithelial-to-mesenchymal signaling in pancreatic development. Dev. Biol. 399, 204–217. doi:10.1016/j.ydbio.2014.12.031.

Ahnfelt-Ronne, J., Jorgensen, M.C., Klinck, R., Jensen, J.N., Fuchtbauer, E.M., Deering, T., Macdonald, R.J., Wright, C.V., Madsen, O.D., Serup, P., 2012. Ptf1a-mediated control of Dll1 reveals an alternative to the lateral inhibition mechanism. Development 139, 33–45. doi:10.1242/dev.071761.

Apelqvist, A., Li, H., Sommer, L., Beatus, P., Anderson, D.J., Honjo, T., Hrabe de Angelis, M., Lendahl, U., Edlund, H., 1999. Notch signalling controls pancreatic cell differentiation. Nature 400, 877–881. doi:10.1038/23716.

Bai, G., Sheng, N., Xie, Z., Bian, W., Yokota, Y., Benezra, R., Kageyama, R., Guillemot, F., Jing, N., 2007. Id sustains Hes1 expression to inhibit precocious neurogenesis by releasing negative autoregulation of Hes1. Dev. Cell 13, 283–297. doi:10.1016/j.devcel.2007.05.014.

Bankaitis, E.D., Bechard, M.E., Wright, C.V., 2015. Feedback control of growth, differentiation, and morphogenesis of pancreatic endocrine progenitors in an epithelial plexus niche. Genes Dev. 29, 2203–2216. doi:10.1101/gad.267914.115.

Beucher, A., Martin, M., Spenle, C., Poulet, M., Collin, C., Gradwohl, G., 2012. Competence of failed endocrine progenitors to give rise to acinar but not ductal cells is restricted to early pancreas development. Dev. Biol. 361, 277–285. doi:10.1016/j.ydbio.2011.10.025.

Bhushan, A., Itoh, N., Kato, S., Thiery, J.P., Czernichow, P., Bellusci, S., Scharfmann, R., 2001. Fgf10 is essential for maintaining the proliferative capacity of epithelial progenitor cells during early pancreatic organogenesis. Development 128, 5109–5117.

Bone, R.A., Bailey, C.S., Wiedermann, G., Ferjentsik, Z., Appleton, P.L., Murray, P.J., Maroto, M., Dale, J.K., 2014. Spatiotemporal oscillations of Notch1, Dll1 and NICD are coordinated across the mouse PSM. Development 141, 4806–4816. doi:10.1242/dev.115535.

Bray, S.J., 2006. Notch signalling: a simple pathway becomes complex. Nat. Rev. Mol. Cell. Biol. 7, 678–689. doi:10.10387/nrm2009.

Cano, D.A., Soria, B., Martin, F., Rojas, A., 2014. Transcriptional control of mammalian pancreas organogenesis. Cell. Mol. Life. Sci. 71, 2383–2402. doi:10.1007/s00018-013-1510-2.

Castro, D.S., Skowronska-Krawczyk, D., Armant, O., Donaldson, I.J., Parras, C., Hunt, C., Critchley, J.A., Nguyen, L., Gossler, A., Gottgens, B., Matter, J.M., Guillemot, F., 2006. Proneural bHLH and Brn proteins coregulate a neurogenic program through cooperative binding to a conserved DNA motif. Dev. Cell. 11, 831–844. doi:10.1016/j.devcel.2006.10.006.

de Back, W., Zhou, J.X., Brusch, L., 2013. On the role of lateral stabilization during early patterning in the pancreas. J. R. Soc. Interface 10. 20120766 doi:10.1098/rsif.2012.0766.

Gasa, R., Mrejen, C., Leachman, N., Otten, M., Barnes, M., Wang, J., Chakrabarti, S., Mirmira, R., German, M., 2004. Proendocrine genes coordinate the pancreatic islet differentiation program in vitro. Proc. Natl. Acad. Sci. USA 101, 13245–13250. doi:10.1073/pnas.0405301101.

Gillespie, D.T., 2000. The chemical Langevin equation. J. Chem. Phys. 113, 297–306. doi:10.1063/1.481811.

Gittes, G.K., 2009. Developmental biology of the pancreas: a comprehensive review. Dev. Biol. 326, 4–35. doi:10.1016/j.ydbio.2008.10.024.

Golson, M.L., Loomes, K.M., Oakey, R., Kaestner, K.H., 2009a. Ductal malformation and pancreatitis in mice caused by conditional Jag1 deletion. Gastroenterology 136, 1761–1771. e1, doi:10.1053/j.gastro.2009.01.040.

Golson, M.L., Le Lay, J., Gao, N., Bramswig, N., Loomes, K.M., Oakey, R., May, C.L., White, P., Kaestner, K.H., 2009b. Jagged1 is a competitive inhibitor of Notch signaling in the embryonic pancreas. Mech. Dev. 126, 687–699. doi:10.1016/j.mod.2009.05.005.

Gouzi, M., Kim, Y.H., Katsumoto, K., Johansson, K., Grapin-Botton, A., 2011. Neurogenin3 initiates stepwise delamination of differentiating endocrine cells during pancreas development. Dev. Dyn. 240, 589–604. doi:10.1002/dvdy.22544.

Gradwohl, G., Dierich, A., LeMeur, M., Guillemot, F., 2000. Neurogenin3 is required for the development of the four endocrine cell lineages of the pancreas. Proc. Natl. Acad. Sci. USA 97, 1607–1611. doi:10.1073/pnas.97.4.1607.

Gu, G., Dubauskaite, J., Melton, D.A., 2002. Direct evidence for the pancreatic lineage: NGN3+ cells are islet progenitors and are distinct from duct progenitors. Development 129, 2447–2457.

Gu, G., Brown, J.R., Melton, D.A., 2003. Direct lineage tracing reveals the ontogeny of pancreatic cell fates during mouse embryogenesis. Mech. Dev. 120, 35–43. doi:10.1016/S0925-4773(02)00330-1.

Hale, M.A., Swift, G.H., Hoang, C.Q., Deering, T.G., Masui, T., Lee, Y.K., Xue, J., MacDonald, R.J., 2014. The nuclear hormone receptor family member NR5A2 controls aspects of multipotent progenitor cell formation and acinar differentiation during pancreatic organogenesis. Development 141, 3123–3133. doi:10.1242/dev.109405.

Hart, A., Papadopoulou, S., Edlund, H., 2003. Fgf10 maintains notch activation, stimulates proliferation, and blocks differentiation of pancreatic epithelial cells. Dev. Dyn. 228, 185–193. doi:10.1002/dvdy.10368.

Hirata, H., Yoshiura, S., Ohtsuka, T., Bessho, Y., Harada, T., Yoshikawa, K., Kageyama, R., 2002. Oscillatory expression of the bHLH factor Hes1 regulated by a negative feedback loop. Science 298, 840–843. doi:10.1126/science.1074560.

Hoffman, B.G., Zavaglia, B., Witzsche, J., Ruiz de Algara, T., Beach, M., Hoodless, P.A., Jones, S.J., Marra, M.A., Helgason, C.D., 2008. Identification of transcripts with enriched expression in the developing and adult pancreas. Genome Biol. 9, R99. doi:10.1186/gb-2008-9-6-r99.

Hua, H., Zhang, Y.Q., Dabernat, S., Kritzik, M., Dietz, D., Sterling, L., Sarvetnick, N., 2006. BMP4 regulates pancreatic progenitor cell expansion through Id2. J Biol. Chem. 281, 13574–13580. doi:10.1074/jbc.M600526200.

Imayoshi, I., Kageyama, R., 2014. bHLH factors in self-renewal, multipotency, and fate choice of neural progenitor cells. Neuron 82, 9–23. doi:10.1016/j.neuron.2014.03.018.

Jensen, J., 2004. Gene regulatory factors in pancreatic development. Dev. Dyn. 229, 176–200. doi:10.1002/dvdy.10460.

Jensen, J., Pedersen, E.E., Galante, P., Hald, J., Heller, R.S., Ishibashi, M., Kageyama, R., Guillemot, F., Serup, P., Madsen, O.D., 2000. Control of endodermal endocrine development by Hes-1. Nat. Genet. 24, 36–44. doi:10.1038/71657.

Jorgensen, M.C., Ahnfelt-Ronne, J., Hald, J., Madsen, O.D., Serup, P., Hecksher-Sorensen, J., 2007. An illustrated review of early pancreas development in the mouse. Endocr. Rev. 28, 685–705. doi:10.1210/er.2007-0016.

Kobayashi, T., Kageyama, R., 2014. Expression dynamics and functions of Hes factors in development and diseases. Curr. Top. Dev. Biol. 110, 263–283. doi:10.1016/B978-0-12-405943-6.00007-5.

Kobayashi, T., Mizuno, H., Imayoshi, I., Furusawa, C., Shirahige, K., Kageyama, R., 2009. The cyclic gene Hes1 contributes to diverse differentiation responses of embryonic stem cells. Genes Dev. 23, 1870–1875. doi:10.1101/gad.1823109.

Lee, J.C., Smith, S.B., Watada, H., Lin, J., Scheel, D., Wang, J., Mirmira, R.G., German, M.S., 2001. Regulation of the pancreatic pro-endocrine gene neurogenin3. Diabetes 50, 928–936. doi:10.2337/diabetes.50.5.928.

Lewis, J., 2003. Autoinhibition with transcriptional delay: a simple mechanism for the zebrafish somitogenesis oscillator. Curr. Biol. 13, 1398–1408. doi:10.1016/S0960-9822(03)00534-7.

Maruhashi, M., Van De Putte, T., Huylebroeck, D., Kondoh, H., Higashi, Y., 2005. Involvement of SIP1 in positioning of somite boundaries in the mouse embryo. Dev. Dyn. 234, 332–338. doi:10.1002/dvdy.20546.

Masui, T., Long, Q., Beres, T.M., Magnuson, M.A., MacDonald, R.J., 2007. Early pancreatic development requires the vertebrate suppressor of hairless (RBPJ) in the PTF1 bHLH complex. Genes Dev. 21, 2629–2643. doi:10.1101/gad.1575207.

Miyatsuka, T., Kosaka, Y., Kim, H., German, M.S., 2011. Neurogenin3 inhibits proliferation in endocrine progenitors by inducing Cdkn1a. Proc. Natl. Acad. Sci. USA 108, 185–190. doi:10.1073/pnas.1004842108.

Monk, N.A., 2003. Oscillatory expression of Hes1, p53, and NF-kappaB driven by transcriptional time delays. Curr. Biol. 13, 1409–1413. doi:10.1016/S0960-9822(03)00494-9.

Murray, J.D., 2002. Mathematical Biology, (third ed.) Springer-Verlag, New York.

Nam, Y., Sliz, P., Pear, W.S., Aster, J.C., Blacklow, S.C., 2007. Cooperative assembly of higher-order Notch complexes functions as a switch to induce transcription. Proc. Natl. Acad. Sci. USA 104, 2103–2108. doi:10.1073/pnas.0611092104.

Newman, S.A., Bhat, R., 2009. Dynamical patterning modules: a “pattern language” for development and evolution of multicellular form. Int. J. Dev. Biol. 53, 693–705. doi:10.1387/ijdb.072481sn.

Norgaard, G.A., Jensen, J.N., Jensen, J., 2003. FGF10 signaling maintains the pancreatic progenitor cell state revealing a novel role of Notch in organ development. Dev. Biol. 264, 323–338. doi:10.1016/j.ydbio.2003.08.013.

Pan, F.C., Wright, C., 2011. Pancreas organogenesis: from bud to plexus to gland. Dev. Dyn. 240, 530–565. doi:10.1002/dvdy.22584.

Philpott, A., Winton, D.J., 2014. Lineage selection and plasticity in the intestinal crypt. Curr. Opin. Cell Biol. 31, 39–45. doi:10.1016/j.ceb.2014.07.002.

Rajagopal, J., Carroll, T.J., Guseh, J.S., Bores, S.A., Blank, L.J., Anderson, W.J., Yu, J., Zhou, Q., McMahon, A.P., Melton, D.A., 2008. Wnt7b stimulates embryonic lung growth by coordinately increasing the replication of epithelium and mesenchyme. Development 135, 1625–1634. doi:10.1242/dev.015495.

Rida, P.C., Le Minh, N., Jiang, Y.J., 2004. A Notch feeling of somite segmentation and beyond. Dev. Biol. 265, 2–22. doi:10.1016/j.ydbio.2003.07.003.

Roark, R., Itzhaki, L., Philpott, A., 2012. Complex regulation controls Neurogenin3 proteolysis. Biol. Open 1, 1264–1272. doi:10.1242/bio.20121750.

Rukstalis, J.M., Habener, J.F., 2007. Snail2, a mediator of epithelial-mesenchymal transitions, expressed in progenitor cells of the developing endocrine pancreas. Gene Expr. Patterns 7, 471–479. doi:10.1016/j.modgep.2006.11.001.

Rukstalis, J.M., Habener, J.F., 2009. Neurogenin3: a master regulator of pancreatic islet differentiation and regeneration. Islets 1, 177–184. doi:10.4161/isl.1.3.9877.

Schaffter, T., 2010. Numerical Integration of SDEs: A Short Tutorial. Swiss Federal Institute of Technology in Lausanne (EPFL) Technical Report LIS-REPORT-2010-001.

Shao, L., Moloney, D.J., Haltiwanger, R., 2003. Fringe modifies O-fucose on mouse Notch1 at epidermal growth factor-like repeats within the ligand-binding site and the Abruptex region. J. Biol. Chem. 278, 7775–7782. doi:10.1074/jbc.M212221200.

Shih, H.P., Wang, A., Sander, M., 2013. Pancreas organogenesis: from lineage determination to morphogenesis. Annu. Rev. Cell Dev. Biol. 29, 81–105. doi:10.1146/annurev-cellbio-101512-122405.

Shih, H.P., Kopp, J.L., Sandhu, M., Dubois, C.L., Seymour, P.A., Grapin-Botton, A., Sander, M., 2012. A Notch-dependent molecular circuitry initiates pancreatic endocrine and ductal cell differentiation. Development 139, 2488–2499. doi:10.1242/dev.078634.

Shimojo, H., Ohtsuka, T., Kageyama, R., 2008. Oscillations in notch signaling regulate maintenance of neural progenitors. Neuron 58, 52–64. doi:10.1016/j.neuron.2008.02.014.

Shimojo, H., Ohtsuka, T., Kageyama, R., 2011. Dynamic expression of notch signaling genes in neural stem/progenitor cells. Front Neurosci. 5, 78. doi:10.3389/fnins.2011.00078.

Shimojo, H., Isomura, A., Ohtsuka, T., Kori, H., Miyachi, H., Kageyama, R., 2016. Oscillatory control of Delta-like1 in cell interactions regulates dynamic gene expression and tissue morphogenesis. Genes Dev. 30, 102–116. doi:10.1101/gad.270785.115.

Sprinzak, D., Lakhanpal, A., Lebon, L., Santat, L.A., Fontes, M.E., Anderson, G.A., Garcia-Ojalvo, J., Elowitz, M.B., 2010. Cis-interactions between Notch and Delta generate mutually exclusive signalling states. Nature 465, 86–90. doi:10.1038/nature08959.

Svensson, P., Bergqvist, I., Norlin, S., Edlund, H., 2009. MFng is dispensable for mouse pancreas development and function. Mol. Cell Biol. 29, 2129–2138. doi:10.1128/MCB.01644-08.

Tiedemann, H.B., Schneltzer, E., Zeiser, S., Hoesel, B., Beckers, J., Przemeck, G.K., Hrabe de Angelis, M., 2012. From dynamic expression patterns to boundary formation in the presomitic mesoderm. PLoS Comput. Biol. 8, e1002586. doi:10.1371/journal.pcbi.1002586.

Tiedemann, H.B., Schneltzer, E., Zeiser, S., Rubio-Aliaga, I., Wurst, W., Beckers, J., Przemeck, G.K., Hrabe de Angelis, M., 2007. Cell-based simulation of dynamic expression patterns in the presomitic mesoderm. J. Theor. Biol. 248, 120–129. doi:10.1016/j.jtbi.2007.05.014.

Villasenor, A., Chong, D.C., Henkemeyer, M., Cleaver, O., 2010. Epithelial dynamics of pancreatic branching morphogenesis. Development 137, 4295–4305. doi:10.1242/dev.052993.

Villasenor, A., Marty-Santos, L., Dravis, C., Fletcher, P., Henkemeyer, M., Cleaver, O., 2012. EphB3 marks delaminating endocrine progenitor cells in the developing pancreas. Dev. Dyn. 241, 1008–1019. doi:10.1002/dvdy.23781.

Volckaert, T., De Langhe, S.P., 2015. Wnt and FGF mediated epithelial-mesenchymal crosstalk during lung development. Dev. Dyn. 244, 342–366. doi:10.1002/dvdy.24234.

Willmann, S.J., Mueller, N.S., Engert, S., Sterr, M., Burtscher, I., Raducanu, A., Irmler, M., Beckers, J., Sass, S., Theis, F.J., Lickert, H., 2016. The global gene expression profile of the secondary transition during pancreatic development. Mech. Dev. 139, 51–64. doi:10.1016/j.mod.2015.11.004.

Yu, H., Shen, Y., Hong, J., Xia, Q., Zhou, F., Liu, X., 2015. The contribution of TGF-beta in epithelial-mesenchymal transition (EMT): down-regulation of E-cadherin via snail. Neoplasma 62, 1–15. doi:10.4149/neo_2015_002.

Zhou, J.X., Brusch, L., Huang, S., 2011. Predicting pancreas cell fate decisions and reprogramming with a hierarchical multi-attractor model. PLoS One 6, e14752. doi:10.1371/journal.pone.0014752.

Zhou, Q., Law, A.C., Rajagopal, J., Anderson, W.J., Gray, P.A., Melton, D.A., 2007. A multipotent progenitor domain guides pancreatic organogenesis. Dev. Cell 13, 103–114. doi:10.1016/j.devcel.2007.06.001.